

# Electrochemical properties of perovskite and $A_2MO_4$ -type oxides used as cathodes in protonic ceramic half cells

J. Dailly · F. Mauvy · M. Marrony · M. Pouchard · Jean-Claude Grenier

Received: 11 June 2010 / Revised: 30 August 2010 / Accepted: 1 September 2010 / Published online: 24 September 2010  
© Springer-Verlag 2010

**Abstract** Three selected materials have been prepared and shaped as cathode of half cells using the proton-conducting electrolyte  $BaCe_{0.9}Y_{0.1}O_{3-\delta}$  (BCY10): two perovskite compounds,  $Ba_{0.5}Sr_{0.5}Co_{0.8}Fe_{0.2}O_{3-\delta}$  (BSCF) and  $La_{0.6}Sr_{0.4}Fe_{0.8}Co_{0.2}O_{3-\delta}$  (LSFC), and the praseodymium nickelate  $Pr_2NiO_{4+\delta}$  (PRN) having the  $K_2NiF_4$ -type structure. The electrochemical properties of these compounds have been studied under zero current conditions (two-electrode cell) and under polarization (three-electrode cell). Their measured area-specific resistances were about  $1\text{--}2 \Omega \text{ cm}^2$  at  $600 \text{ }^\circ\text{C}$ . Under direct current polarization, it appears that the three compounds show almost similar values of current densities at  $625 \text{ }^\circ\text{C}$ ; however, at lower temperatures, BSCF appears to be the most efficient cathode material.

**Keywords** SOFC- $H^+$  · Perovskite ·  $K_2NiF_4$ -type oxides · Cathode material · Impedance spectroscopy

## Introduction

Conventional solid oxide fuel cells (SOFCs) operate at high temperature, around  $800\text{--}1000 \text{ }^\circ\text{C}$ , which causes damages in long-term applications and requires expansive materials

for cell fabrication. Operating at lower temperatures ( $500\text{--}700 \text{ }^\circ\text{C}$ ) is obviously beneficial in terms of durability and cost (classical materials can be used) for these systems. However, at such temperatures, it is crucial first to improve the ionic conductivity of the electrolyte and secondly to enhance the kinetics of the electrode reactions, especially at the cathode side.

In this way, great efforts are devoted to develop new systems based on protonic conducting thin ceramic membranes (SOFC- $H^+$ ) capable of operating around  $500\text{--}600 \text{ }^\circ\text{C}$  [1–5]. However, this kind of fuel cells requires new cathode materials; they should be chemically stable at high temperature in the presence of water which is formed at the cathode side and should also show good electrocatalytic properties for the oxygen reduction.

Up to now, several mixed ionic and electronic conducting (MEIC) oxides have been investigated as SOFC- $H^+$  cathodes; they are mainly ferrites and cobaltites with perovskite or double perovskite-type structures,  $K_2NiF_4$ -type nickelates, and layered cobaltites  $Ca_3Co_4O_{9-\delta}$  [4–9]. We recently studied various MEIC oxides with the aim to select the best ones as cathode [10].

We found that most of them are not significantly affected by moist atmosphere. According to TGA experiments, it was observed that the quantity of inserted water is always small, for instance, less than  $0.03 \text{ mol H}_2\text{O}$  per mole for  $La_2NiO_{4+\delta}$ . In the same way, the electrical conductivity is not changed by the presence of water in the surrounding atmosphere or even by some hydration of the materials, which means the mixed valence of the cations and then the concentration of holes remain unchanged [10]. In addition, their electrochemical characteristics were determined on symmetrical half cells under zero direct current (dc) conditions. The various contributions of the impedance spectroscopy diagrams were assigned to different electro-

---

This article is dedicated to Professor Robert Schöllhorn in celebration of his 75th Birthday, from colleagues of Bordeaux (France).

---

J. Dailly · F. Mauvy · M. Pouchard · J.-C. Grenier (✉)  
CNRS, Université de Bordeaux, ICMCB,  
87, Av. du Dr Schweitzer,  
33608 Pessac, France  
e-mail: grenier@icmcb-bordeaux.cnrs.fr

M. Marrony  
EDF- EIfER Emmy-Noether-Strasse 11,  
76131 Karlsruhe, Germany

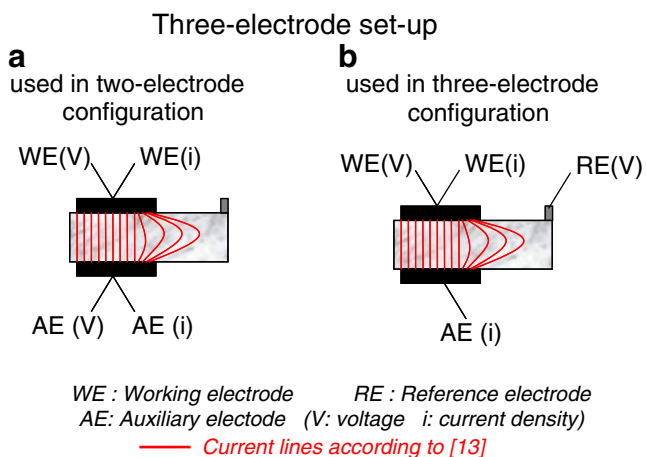


**Fig. 1** Schematic representation of the two configurations used for EIS measurements: **a** two-electrode symmetrical configuration, **b** three-electrode cell

chemical processes; however, the electrode reaction mechanism was not elucidated. Whether the cathode materials exhibit some protonic conductivity or not remains an open question. On the basis of these results, the cathodic area-specific resistance (so called ASR) values evidenced three compounds to show the best promising performances: they are two perovskites,  $\text{Ba}_{0.5}\text{Sr}_{0.5}\text{Co}_{0.8}\text{Fe}_{0.2}\text{O}_{3-\delta}$  (BSCF) and  $\text{La}_{0.6}\text{Sr}_{0.4}\text{Fe}_{0.8}\text{Co}_{0.2}\text{O}_{3-\delta}$  (LSFC) and the praseodymium nickelate  $\text{Pr}_2\text{NiO}_{4+\delta}$  (PRN).

In this work, we report the electrochemical properties of these three compounds under polarization using three-electrode symmetrical half cells with  $\text{BaCe}_{0.9}\text{Y}_{0.1}\text{O}_{3-\delta}$  (BCY10) as proton-conducting electrolyte [11]; the aim of this study is to select the most efficient cathode material.

## Experimental

For this study, the half cells were made of an electrolyte ceramic membrane and two symmetrical electrodes.

### Preparation of cell materials and chemical reactivity

The electrolyte is the yttrium-doped barium cerate, BCY10; fine powder with a particle size distribution of  $D_{V(0.5)} = 0.3 \mu\text{m}$  was supplied by Marion Technology Co. and used as received. The powder (1.5 g) was first shaped as pellets ( $\varnothing = 16 \text{ mm}$ ) under 2 T uniaxial force; then these pellets were isostatically pressed under 300 MPa and sintered at  $1,400 \text{ }^\circ\text{C}$  for 4–10 h. The obtained ceramic membranes had a final density of about 95% and a thickness of 1 mm. Their surface was roughened with a # 600 grit paper and then cleaned with ethanol solution.

For the electrodes, LSFC, BSCF, and PRN, powders were prepared by the modified Pechini method [12]. The

required amounts of the starting oxides were first dissolved into 12 M nitric acid. Citric acid was then added to the solution in a large excess, and the resultant clear solution was then slowly heated up to  $120 \text{ }^\circ\text{C}$  to obtain a viscous brown gel which was charred at  $600 \text{ }^\circ\text{C}$ . A final heating step at  $1,000 \text{ }^\circ\text{C}$ , for 12 h, led the required compounds. XRD patterns confirmed the as-prepared phases to be pure.

For intermediate temperature fuel cell application, it is important to study the chemical reactivity of the electrode materials with electrolyte with respect to the long-term performances. It is well known that electrodes can react with electrolyte at high temperatures to form new phases that, when they are insulating, act as blocking interface, leading to an increase of the polarization resistance. Electrode and electrolyte powders were intimately mixed together (1:1 mass ratio) and pressed to form pellets. These pellets were sintered at  $1,200 \text{ }^\circ\text{C}$  for 1 h (as for the electrode sintering) and aged at  $650 \text{ }^\circ\text{C}$ , in wet air, for 3 weeks. The mixture was then analyzed by X-ray diffraction and scanning electron microscopy (SEM). Results demonstrated that, at the sintering temperature, the reactivity was negligible for the perovskite compounds (LSFC and BSCF) whereas it was observed for ( $\text{Pr}_2\text{NiO}_{4+\delta}$ /BCY10) the formation of a small amount of perovskite-type phase. The aging did not reveal significant reactivity of the three compounds with the electrolyte.

### Preparation of symmetrical half cells

The symmetrical half cells consisted in the as-prepared electrolyte pellets ( $\varnothing = 16 \text{ mm}$ ) of  $\text{BaCe}_{0.9}\text{Y}_{0.1}\text{O}_{3-\delta}$  on which electrodes made of investigated materials were deposited by screen printing. The standard ink was prepared starting from electrode powder with a particle size distribution (PSD) of about  $0.5 \mu\text{m}$ . Then, electrodes

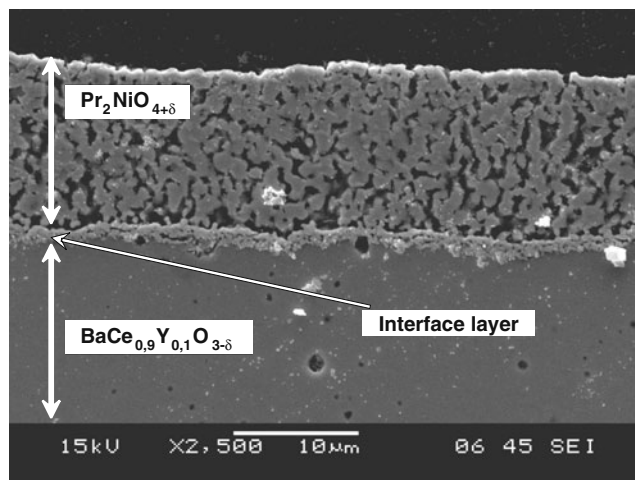


**Fig. 2** Typical micrograph of a half cell: example of the  $\text{Pr}_2\text{NiO}_{4+\delta}$ / $\text{BaCe}_{0.9}\text{Y}_{0.1}\text{O}_{3-\delta}$  cell

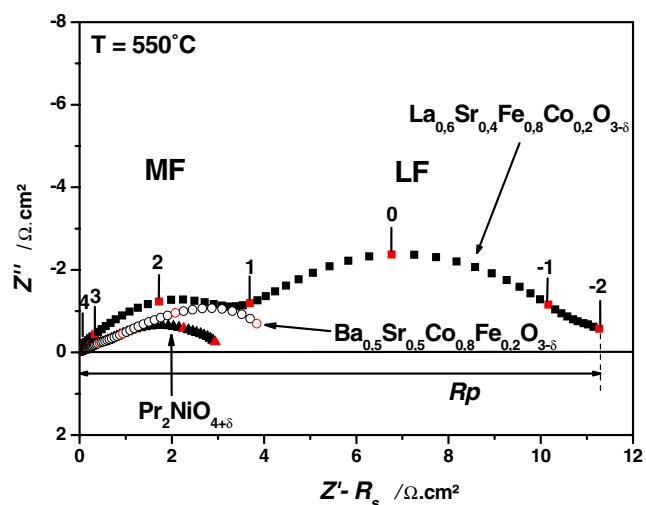


**Fig. 3** Typical impedance diagrams obtained at  $T=550\text{ }^{\circ}\text{C}$ , under wet air, for symmetrical cells, LSFC/BCY10, BSCF/BCY10, and PRN/BCY10

were screen-printed on half the surface of both sides of the BCY10 pellet in symmetrical configuration whatever the used measurement method (two or three electrodes as shown in Fig. 1).

Specific high-temperature sintering was required in order to obtain a good adherence of the cathode layer on the electrolyte, which is particularly important in order to provide a good quality of the interface electrode/electrolyte while avoiding excessive reaction between materials. In this work, the cells were first slowly heated up to  $400\text{ }^{\circ}\text{C}$  in order to burn out the organic binders and then sintered at  $1,200\text{ }^{\circ}\text{C}$  for 1 h. Figure 2 shows the SEM image of a typical  $\text{Pr}_2\text{NiO}_{4+\delta}$  prepared electrode. It can be seen that the electrode microstructure appears uniform and shows good adherence with the BCY10 pellet. From the cross section, one can estimate that the mean particle size is about  $1\text{ }\mu\text{m}$  and the thickness of the electrode is about  $30\text{ }\mu\text{m}$  with a porosity of 35–40%, calculated using ImageJ software. The half cells are placed into an alumina ceramic support and a Pt mesh is used as the current collector.

Electrochemical impedance spectroscopy (EIS) measurements were performed either in two-electrode configuration (zero dc conditions, Fig. 1a) or in three-electrode configuration (under dc polarization, Fig. 1b). For this geometry, the reference electrode was made of Pt paste painted on the same side of the working electrode, at a distance of the cathode over five times of the thickness of the pellets [13]. All the electrochemical experiments were performed from 800 to  $300\text{ }^{\circ}\text{C}$ , under moist flowing air ( $P_{\text{H}_2\text{O}} = 0.032\text{ atm}$ ), at thermodynamical equilibrium. The impedance diagrams were obtained using an Autolab PGSTAT302 Frequency Response Analyzer. The data obtained were fitted using the ZView software.

## Results and discussion

Electrochemical measurements (two-electrode cell) under zero dc conditions

EIS measurements were performed for symmetrical electrode/BCY10/electrode cells under zero dc current conditions, at thermodynamical equilibrium (at given temperature, in air). Typical Nyquist plots obtained at  $550\text{ }^{\circ}\text{C}$  for the three compounds are shown in Fig. 3. Several contributions can be evidenced; all data were fitted on the basis of an equivalent circuit constituted of two resistance-constant-phase elements ( $R\text{-CPE}$ ) in parallel, associated in series. In order to easily compare the polarization resistances of the electrodes, the series resistance of the cells ( $R_s$ , at high frequencies) was subtracted from the EIS data.

Concerning the electrode process, two different contributions were identified on the impedance diagrams (Fig. 3); referring to previous works [10, 14], they can be interpreted as follows: (1) the first semi-circle in the middle-frequency regime (MF) is assigned to the transfer of  $\text{H}^+$  ions from the electrolyte to the electrode on the basis of its small capacitance, (2) the large depressed arc at low frequency (LF impedance) is postulated to characterize oxygen adsorption/dissociation steps overlapped with diffusion processes. According to this assignment, the polarization resistance  $R_p$  is deduced from the sum of both resistances  $R_{\text{MF}}$  and  $R_{\text{LF}}$  corresponding to the MF and LF contributions.

The thermal variations of the ASR of the electrodes, calculated with the relation  $\text{ASR} = R_p \times S/2$ ,  $R_p$  being the difference between low- and high-frequency intercepts of

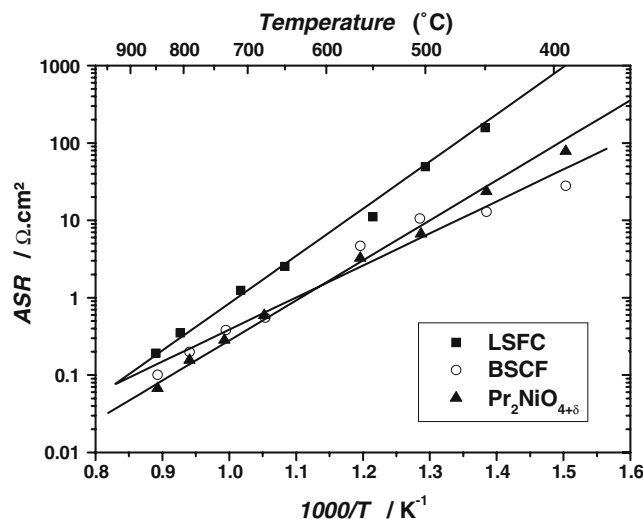


**Fig. 4** Arrhenius plots of cathodic ASRs for the LSFC, BSCF, and PRN electrodes

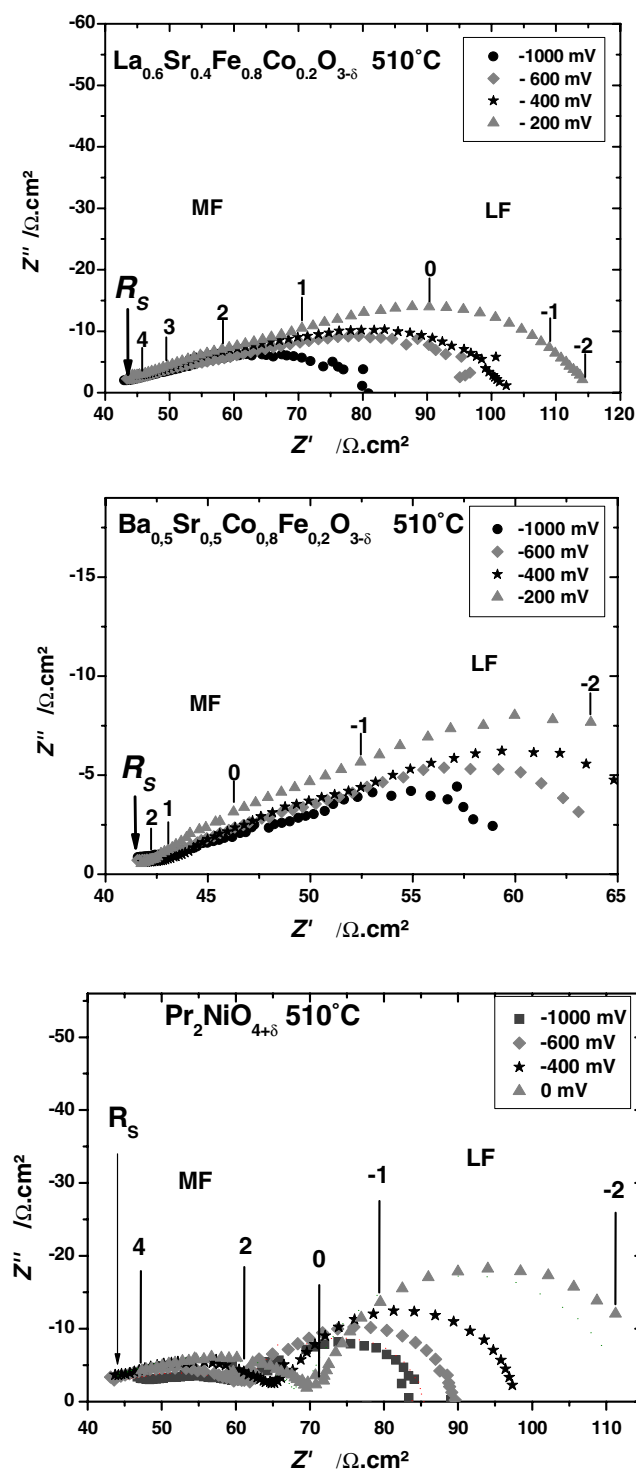


Fig. 5 EIS diagrams recorded with the three-electrode cells under dc polarization at  $T=510\text{ }^{\circ}\text{C}$  (LSFC, BSCF, and PRN as electrode materials and BCY10 as electrolyte)

the impedance diagrams with the real axis (Fig. 3) and  $S$  the electrode surface area ( $S=2\text{ cm}^2$ ), are shown in Fig. 4. Under zero dc bias conditions,  $\text{Pr}_2\text{NiO}_{4+\delta}$  appears to be the electrode having the lowest ASR for temperatures higher

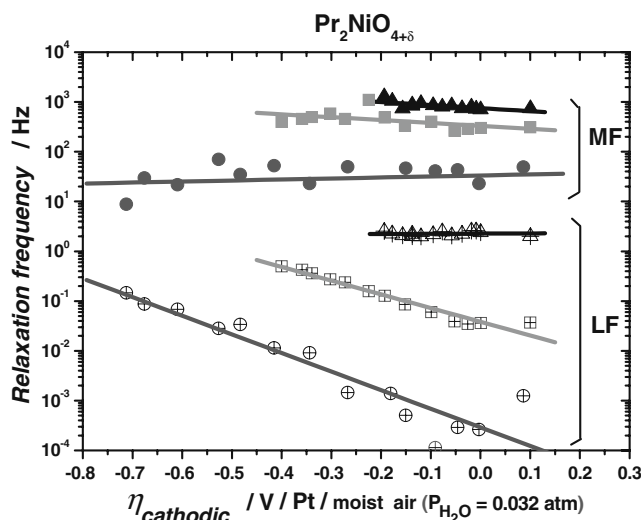


Fig. 6 Relaxation frequencies of  $\text{Pr}_2\text{NiO}_{4+\delta}$  electrode versus overvoltage at  $T=400\text{ }^{\circ}\text{C}$  (circles),  $510\text{ }^{\circ}\text{C}$  (squares), and  $625\text{ }^{\circ}\text{C}$  (triangles)

than  $450\text{ }^{\circ}\text{C}$  whereas  $\text{Ba}_{0.5}\text{Sr}_{0.5}\text{Co}_{0.8}\text{Fe}_{0.2}\text{O}_{3-\delta}$  shows better electrochemical properties for temperatures lower than  $450\text{ }^{\circ}\text{C}$ .

Electrochemical measurements under dc polarization

Under operating conditions, the polarization phenomenon at the cathode is one of the major problems in the field of fuel cells. This study was carried out using the three-electrode setup described in Fig. 2a. The purpose is to measure the working electrode overvoltage under cathodic current conditions and to analyze the various contributions to polarization resistance under current.

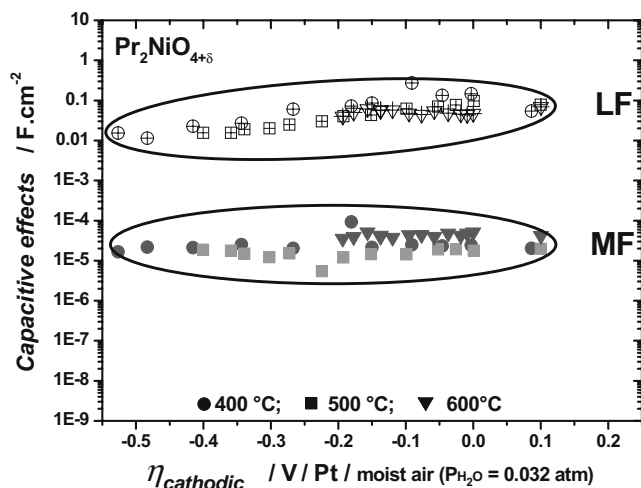


Fig. 7 Capacitive effects versus cathodic overvoltage for the  $\text{Pr}_2\text{NiO}_{4+\delta}$  electrode material at  $T=400, 510,$  and  $625\text{ }^{\circ}\text{C}$

**Table 1** MF and LF capacitance values of the  $\text{Pr}_2\text{NiO}_{4+\delta}$ ,  $\text{Ba}_{0.5}\text{Sr}_{0.5}\text{Co}_{0.8}\text{Fe}_{0.2}\text{O}_{3-\delta}$ , and  $\text{La}_{0.6}\text{Sr}_{0.4}\text{Fe}_{0.8}\text{Co}_{0.2}\text{O}_{3-\delta}$  electrodes measured under dc polarization conditions in the temperature range 400–625 °C

Electrode material	$C_{\text{MF}}$ (Fcm <sup>2</sup> )	$C_{\text{LF}}$ (Fcm <sup>2</sup> )
$\text{Pr}_2\text{NiO}_{4+\delta}$	$2 \times 10^{-5}$	0.1–0.01
BSCF	$5 \times 10^{-4}$ – $10^{-4}$	1–0.1
LSFC	$4 \times 10^{-3}$ – $10^{-5}$	$0.01$ – $3 \times 10^{-3}$

*EIS analysis versus cathodic overvoltage*

The electrochemical characterization of the cathode materials was determined from complex impedance diagrams measured under various dc polarizations in the range ( $-1 < E_{\text{WE}} - E_{\text{RE}} < 0 \text{ V/Pt}$ ), under wet air (3.2% of water). Typical impedance diagrams of the three investigated compounds are reported in Fig. 5.

On the basis of the fitted data, relaxation frequencies and associated capacitances have been calculated as well as the various resistances  $R_s$ ,  $R_{\text{MF}}$ , and  $R_{\text{LF}}$ . Their values are directly correlated through the well-known relation  $2\pi \times f \times R \times C = 1$ .

1. Relaxation frequencies

The relaxation frequency is a relevant parameter which does not depend upon the geometrical features of the cell; typical variations of the MF and BF relaxation frequencies as a function of the cathodic overvoltage are reported in Fig. 6 for  $\text{Pr}_2\text{NiO}_{4+\delta}$  as cathode, at three temperatures (400, 510, and 625 °C). As expected, the values of MF and LF frequencies increase with increasing temperature, indicating a thermal activation of the electrode process.

The frequency of LF contribution increases with cathodic voltage at 400 and 510 °C, while it is almost constant at 625 °C. The MF relaxation frequency is almost constant with the overvoltage. It can be deduced that the polarization favors the electrode reaction whereas it has little influence on interfacial phenomena.

A similar feature was also observed for  $\text{Ba}_{0.5}\text{Sr}_{0.5}\text{Co}_{0.8}\text{Fe}_{0.2}\text{O}_{3-\delta}$ . On the other hand, for  $\text{La}_{0.6}\text{Sr}_{0.4}\text{Fe}_{0.8}\text{Co}_{0.2}\text{O}_{3-\delta}$  compound, the values of the MF and LF frequency relaxation also increase with temperature; however, they are almost constant as a function of the overvoltage, whatever the temperature, in the range 400–625 °C.

It clearly appears that the MF contribution frequency does not change with polarization, which is consistent with the fact that this impedance is assigned to the ionic transfer at the interface electrolyte/electrode. Indeed, it is known that this ionic transfer is not significantly influenced by the polarization. On the other hand, the

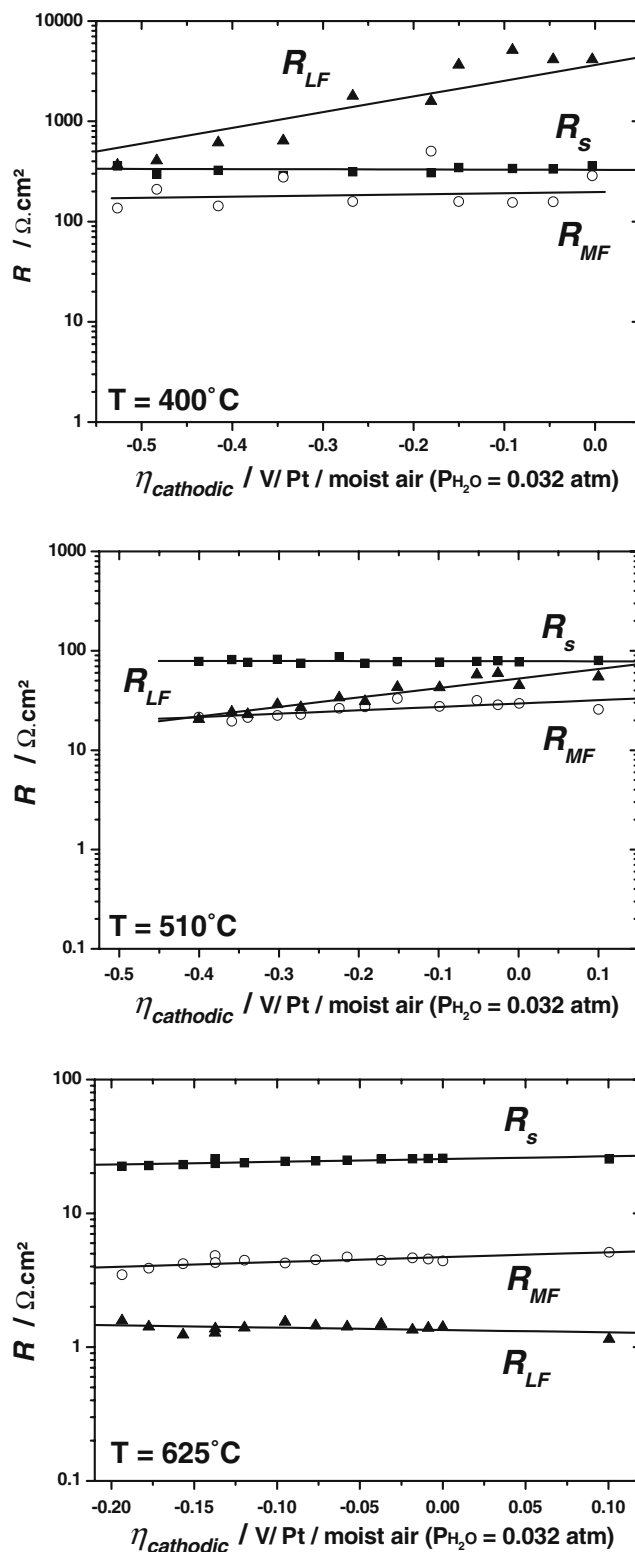


**Fig. 8** Variation of the resistive contributions vs. cathodic overvoltage, at various temperatures, for the  $\text{Pr}_2\text{NiO}_{4+\delta}$  electrode

electrode reaction (LF contribution) is not only improved by the temperature as expected but also by the amplitude of the overvoltage.



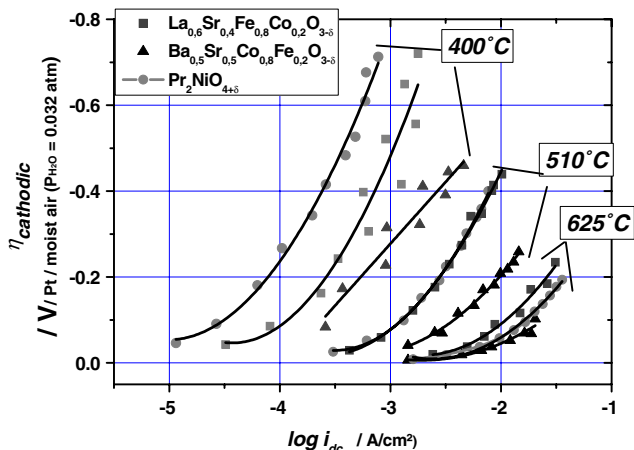


**Fig. 9** Tafel curves of cathodic overvoltage versus Log  $i_{dc}$  for  $\text{La}_{0.6}\text{Sr}_{0.4}\text{Fe}_{0.8}\text{Co}_{0.2}\text{O}_{3-\delta}$ ,  $\text{Pr}_2\text{NiO}_{4+\delta}$ , and  $\text{Ba}_{0.5}\text{Sr}_{0.5}\text{Co}_{0.8}\text{Fe}_{0.2}\text{O}_{3-\delta}$  electrodes ( $T=625, 511, \text{ and } 400\text{ }^\circ\text{C}$ )

2. Capacitive effects

Capacitive effects are also very relevant parameters for characterizing the electrode behavior with regard to specific electrochemical processes. Figure 7 shows the capacitive effects as a function of the overvoltage for the  $\text{Pr}_2\text{NiO}_{4+\delta}$  cathode material, at various temperatures. The capacitance does not depend upon temperature as well as upon overvoltage. A quite similar behavior is observed for  $\text{Ba}_{0.5}\text{Sr}_{0.5}\text{Co}_{0.8}\text{Fe}_{0.2}\text{O}_{3-\delta}$ ; more scattered values are obtained for  $\text{La}_{0.6}\text{Sr}_{0.4}\text{Fe}_{0.8}\text{Co}_{0.2}\text{O}_{3-\delta}$  (Table 1).

From all these results, it is observed that the polarization as well as the temperature does not significantly affect the capacitive effects of the electrodes, which means that these three electrodes remain stable (chemically or electrochemically speaking) in the conditions of our studies ( $0 < \eta \leq 0.5\text{V/Pt}$  under the temperature range  $400\text{--}625\text{ }^\circ\text{C}$ ).

3. Resistances

The variations of the resistances ( $R_S, R_{MF}, R_{LF}$ ) as a function of the overvoltage, at various temperatures, are reported in Fig. 8 for  $\text{Pr}_2\text{NiO}_{4+\delta}$  electrode.

First, it can be noticed that the series resistance  $R_S$ , associated with the electrolyte, does not vary with the

**Table 2** Current density measured with LSFC, PRN, and BSCF at  $\eta=-100\text{ mV/Pt/moist air}$  ( $P_{\text{H}_2\text{O}} = 0.032\text{ atm}$ ) for  $T=625, 511, \text{ and } 400\text{ }^\circ\text{C}$

Electrode material	$i_{dc}$ (mA/cm <sup>2</sup> ), 625 °C, $\eta=-100\text{ mV}$	$i_{dc}$ (mA/cm <sup>2</sup> ), 510 °C, $\eta=-100\text{ mV}$	$i_{dc}$ (mA/cm <sup>2</sup> ), 400 °C, $\eta=-100\text{ mV}$
$\text{La}_{0.6}\text{Sr}_{0.4}\text{Fe}_{0.8}\text{Co}_{0.2}\text{O}_{3-\delta}$	10	1.3	$9.1 \times 10^{-2}$
$\text{Pr}_2\text{NiO}_{4+\delta}$	17	1.3	$2.6 \times 10^{-2}$
$\text{Ba}_{0.5}\text{Sr}_{0.5}\text{Co}_{0.8}\text{Fe}_{0.2}\text{O}_{3-\delta}$	21	3.7	$2.6 \times 10^{-1}$

**Table 3** Exchange current densities measured with LSFC, PRN, and BSCF cathode materials at  $T=625, 510, \text{ and } 400\text{ }^\circ\text{C}$

Electrode material	$i_0$ (mA/cm <sup>2</sup> ), 625 °C	$i_0$ (mA/cm <sup>2</sup> ), 510 °C	$i_0$ (mA/cm <sup>2</sup> ), 400 °C
$\text{La}_{0.6}\text{Sr}_{0.4}\text{Fe}_{0.8}\text{Co}_{0.2}\text{O}_{3-\delta}$	5.8	1.0	0.12
$\text{Pr}_2\text{NiO}_{4+\delta}$	8.1	1.0	0.06
$\text{Ba}_{0.5}\text{Sr}_{0.5}\text{Co}_{0.8}\text{Fe}_{0.2}\text{O}_{3-\delta}$	6.5	2.1	0.17

cathodic overvoltage, indicating that the polarization does not significantly alter the protonic electrolyte membrane, whatever the temperature. As expected, this resistance decreases when temperature increases. The large value of  $R_S$  is the consequence of the thickness of the electrolyte ( $\approx 1\text{ mm}$ ). Similar features were found for the two other half cells with the perovskite-type materials as cathodes.

The study of  $R_{MF}$  and  $R_{LF}$  resistances as a function of overvoltage and temperature allows determining the limiting step of the electrode processes. For  $\text{Pr}_2\text{NiO}_{4+\delta}$ , the  $R_{MF}$  and  $R_{LF}$  resistance values decrease with increasing temperature (Fig. 8), which results from the thermal activation of the electrochemical reactions. One can also notice that the MF resistance is almost constant with the overvoltage whereas the LF resistance decreases with increasing cathode overvoltage; the larger is the decrease, the lower is the temperature. This suggests that the polarization contributes to the improvement of the electrode reaction kinetics, especially at lowest temperatures.

In addition, the  $R_{MF}$  resistance of  $\text{Pr}_2\text{NiO}_{4+\delta}$  material is smaller than the  $R_{LF}$  one at 400 and 510 °C. It can be deduced that the contribution of the electrode reaction is more penalizing at these temperatures while it is the opposite at 600 °C, at which temperature, ionic transfer at the electrode/electrolyte interface becomes more detrimental.

For both perovskite compounds, BSCF and LSFC, similar results were found: the  $R_{MF}$  and  $R_{LF}$  resistance values decrease with increasing temperature. In addition,  $R_{MF}$  contribution does not vary significantly with the cathode overvoltage. Conversely, the cathodic overvoltage again promotes the electrode reaction, but this  $R_{LF}$  contribution remains predominant with respect to the ionic transfer contribution ( $R_{MF}$ ), whatever the temperature. For the perovskite compounds, the LF resistance contribution being the largest one, it can be concluded that the electrode reaction seems to be the limiting step for these electrode materials.

Concerning the resistance measured in the medium-frequency range (MF assigned to interface phenomena), the change with polarization is small while the contribution at low frequencies (LF assigned to electrode reaction) is much

more affected, a significant decrease being observed. This observation is the most obvious for the  $\text{Pr}_2\text{NiO}_{4+\delta}/\text{BaCe}_{0.9}\text{Y}_{0.1}\text{O}_{3-\delta}$  half cell in so far as the contributions are clearly separated.

#### *Polarization curves under cathodic conditions*

The electrochemical performance of an electrode can be estimated from the  $(\eta-i_{\text{dc}})$  curves. Figure 9 shows the Tafel plots of PRN, BSCF, and LSFC for cathodic current densities, under wet air, at various temperatures. The values of current densities  $i_{\text{dc}}$  at given overvoltage cathode,  $\eta=-100$  mV/Pt, value usually chosen for the cathode voltage of a SOFC [15], are reported in Table 2. Whatever the values of overvoltage and temperature, BSCF shows the highest values of current density. It can be mentioned that similar studies have been performed on perovskite compounds  $\text{La}_{1-x}\text{Sr}_x\text{MO}_{3-\delta}$  ( $M=\text{Mn, Co, Fe}$ ) deposited by painting on a proton-conducting electrolyte  $\text{SrCe}_{0.95}\text{Y}_{0.05}\text{O}_{3-\delta}$  [15]. For an overvoltage of  $\eta=-100$  mV/Pt, the highest current density was obtained with the lanthanum ferrite, i.e., 3 mA/cm<sup>2</sup> at 700 °C.

From  $(\eta, \text{Log } i_{\text{dc}})$  curves, the current exchange densities  $i^0$  have been calculated. From the results reported in Table 3, it can be concluded that current exchange densities are of the same order of magnitude (5–6 mA/cm<sup>2</sup> at 625 °C) for LSFC and BSCF compounds and slightly larger for PRN (8.1 mA/cm<sup>2</sup>). At 510 and 400 °C, the BSCF electrode seems to be more efficient than the two other ones.

#### **Conclusion**

On the basis of previous results [10] dealing with oxides for cathodes of protonic ceramic fuel cells, three compounds were selected for further studies: there are two perovskite compounds, BSCF and LSFC, and the praseodymium nickelate PRN having the  $\text{K}_2\text{NiF}_4$ -type structure. They have been synthesized, characterized, and then screen-printed on dense pellets of BCY10 used as proton-conducting electrolyte. Electrochemical experiments on symmetrical half cells were then performed under  $i_{\text{dc}}=0$  conditions (two-electrode cell) and under dc polarization (three-electrode cell).

The ASR were measured, and values of about 1–2  $\Omega\text{cm}^2$  at 600 °C showed these compounds to be promising as SOFC- $\text{H}^+$  cathode. EIS measurements show that the polarization favors the electrode reaction whereas it results in a small influence on interfacial phenomena. It appears that the three compounds show almost similar values of

exchange current densities at 625 °C; however, at lower temperatures, BSCF appears to be the most efficient cathode material.

With respect to the sensitivity of compounds containing alkaline earth elements against  $\text{CO}_2$  or even  $\text{H}_2\text{O}$ , which has been previously reported [16, 17], the praseodymium nickelate was selected for further experiments. A single cell involving an anode-supported cell made of Ni cermet with BCY10 electrolyte and  $\text{Pr}_2\text{NiO}_{4+\delta}$  as cathode has been carried out; a power density of 130 mWcm<sup>-2</sup> was obtained at 923 K [8]. Improving the microstructure of the cathode allowed values to reach up to 180 mWcm<sup>-2</sup> recently [18].

**Acknowledgements** The authors acknowledge the financial support from the “Agence Nationale de la Recherche” under the Tectonic project (ANR-05-PANH-01503) and from the French Agency “ADEME.”

#### **References**

1. Coors WG (2003) *J Power Sources* 118:150
2. Iwahara H, Asakura Y, Katahira K, Tanaka M (2004) *Solid State Ionics* 168:299–310
3. Yamaguchi S, Yamamoto S, Shishido T, Omori M, Okudo A (2004) *J Power Sources* 129:4
4. D’Epifanio A, Fabbri E, Liccocia S, Traversa E (2008) *Fuel Cells* 8:69
5. Ranran P, Yan W, Lizhai Y, Mao Z (2006) *Solid State Ionics* 177:389
6. Lin B, Ding H, Dong Y, Wang S, Zhang X, Fang D, Meng G (2009) *J Power Sources* 186:58–61
7. Ding H, Xue X (2010) *Int J Hydrogen Energy* 35:2486–2490
8. Taillades G, Dailly J, Taillades-Jacquini M, Mauvy F, Essouhmi A, Marrony M, Lalanne C, Fourcade S, Jones DJ, Grenier J-C, Rozière J (2010) *Fuel Cells* 10(1):166
9. Ben Yahia H, Mauvy F, Grenier J-C (2010) *J Solid State Chem* 183:527–531
10. Dailly J, Fourcade S, Largeteau A, Mauvy F, Grenier J-C, Marrony M (2010) *Electrochim Acta* 55:5847
11. Kreuer KD (2003) *Annu Rev Mater Res* 33:333
12. Courty P, Ajour H, Marcilly C, Delmon B (1973) *Powder Technol* 7:21–38
13. Cimenti M, Co AC, Birss VI, Hill JM (2007) *Fuel Cells* 07-5:364–376
14. Zhao H, Mauvy F, Bassat J-M, Fourcade S, Lalanne C, Boehm E, Grenier J-C (2008) *Solid State Ionics* 179:2000–2005
15. Yamaura H, Ikuta T, Yahiro H, Okada G (2005) *Solid State Ionics* 176:269–274
16. Yan A, Yang M, Hou Z, Dong Y, Cheng M (2008) *J Power Sources* 185:76–84
17. Yan A, Cheng M, Dong Y, Yang W, Maragou V, Song S, Tsiakaras P (2006) *Appl Catal B* 66:64–71
18. Grimaud A, Mauvy F, Bassat J-M, Grenier J-C, Dailly J, Marrony M (2010) *Proceedings of E-MRS 2010 Spring Meeting*, June 8–10, Strasbourg, France